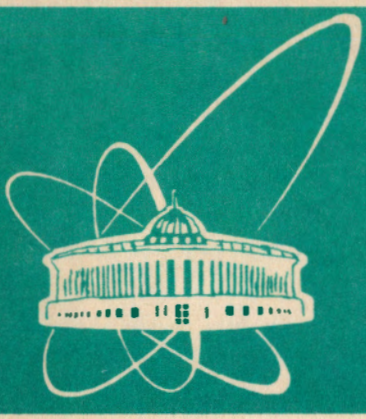

сообщения
объединенного
института
ядерных
исследований
дубна

E1-93-20

B.V.Batyunya, I.V.Boguslavsky, D.Bruncko[1], C.Coca[2],
I.M.Gramenitsky, K.S.Medved, T.Ponta[2], I.B.Simkovicova

NEUTRAL STRANGE PARTICLE YIELDS AND PRODUCTION RATIOS IN ANTIDEUTERON-NUCLEI INTERACTIONS AT 12.2 GEV/C

[1]Institute of Experimental Physics, Slovak Acad. of Sciences, Kosice, Slovakia
[2]Central Institute of Physics, Bucharest, Romania

1993

1. Introduction

The behavior of nuclei at high density and temperature is still relatively unknown. There are some possibilities to study nuclear matter excitation processes in antinucleon-nucleus interactions due to the ability of antinucleons to annihilate in nuclear matter delivering considerable energy into a nucleus. With energies of a few GeV, antiprotons may release their entire energy inside a nucleus and heat up a tiny domain to a high temperature. One of the signals for such a process is expected to be the enhanced strange particle production [1, 2].

At present, there are only several results on neutral strange particle production in $\bar{p}$-nucleus interactions in the momentum range of 0–4 GeV/c [3–16]. The results of all these investigations have shown that there are some processes in antiproton–nuclei collisions that increase greatly the Λ-production without K_s° yield reducing, if to be compared with the corresponding values for $\bar{p}p$ interactions.

Various models have been used to explain the high Λ yield. In [2] the strangeness enhancement was considered to be the result of supercooled quark-gluon plasma formation, whereas in [18] this phenomenon explained in terms of multinucleon absorption reactions.

But it was also demonstrated that the data on Λ and K_s° production in $\bar{p}$-interactions with heavy targets, might be explained within the framework of the IntraNuclear Cascade models [12, 19, 20]. These models have been used to reproduce the Λ production characteristics under the assumption that strangeness is produced in conventional $\bar{N}N$ processes and then redistributed in secondary meson rescattering.

One can find the review of the experimental situation in [17].

The 2-m HBC "Ludmila" was exposed to a 12.2 GeV/c antideuteron beam at the Serpukhov accelerator. The main task of the experiment was to study the multinucleon effects in the antideuteron-deuteron interactions. Besides, the construction of the target also allowed one to observe interactions of antideuterons with the heavier nuclei. Naturally, the idea appeared to watch the behavior of neutral strange particle production in $\bar{d}$-nuclei reactions, for to see if there were any effects similar to those found in antiproton interactions.

In this paper we present the experimental data on Λ and K°_{s} inclusive yields and Λ/K°_{s} production ratios in antideuteron – deuteron,antideuteron – carbon and antideuteron – lead interactions. This publication is also concentrated on the methodical peculiarities of data handling procedures.

2. Antideuteron beam and experimental arrangement

Antideuteron beam was created irradiating a copper target with proton beam at 70 GeV. A two-stage scheme of separation [22] was used to suppress the hadron background. The maximum of the secondary antideuterons yield lies in the momentum interval of (10–13) GeV/c. In this case the yield ratio of negative pions, antiprotons, and antideuterons is approximately equal to $1{:}10^{-3}{:}10^{-6}$, respectively [23]. During the experimental runs the intensity of antideuterons was about 0.5 per picture at the antideuteron momentum of 12.2 GeV/c.

Filled with liquid deuterium, the internal track-sensitive target was installed inside the chamber, while the $\bar{d}d$ experiment. The target was made of the transparent material – lexan (thermoplastic polycarbonate $H_{14}C_{16}O_3$), partially surrounded with lead plates. The construction of the target allows one to observe and measure the interactions of beam antideuterons in lexan target walls and lead plates (see Fig. 1). The lexan plate was 12 mm thick and lead plate – 3 mm. The magnetic field at the center of the chamber was 26 kG. You can find more details about the experiment in [24].

3. Event handling procedure

The film material was scanned visually on projection tables. The total sample was of 72K pictures. The antideuteron-deuteron interactions have been also registered inside the deuterium target during the previous runs. The events were searched for twice, the scanning efficiency was found as 0.97. The number of registered $\bar{d}A$ events with/without vees is presented in Table II.

Tracks of the primary interaction and vees were measured with manual PUOS digitizers in three views. Each event with, at least, one associated V° candidate, was fully measured; the geometric reconstruction of the tracks as well as neutral strange particle fitting was performed by the standard HYDRA program chain.

The position of the invisible vertex inside the plates was calculated interpolating the charged secondary tracks. This procedure allows one not only to make a three - constraint fit of neutral particle but also to check whether the interaction point lies inside the lexan or lead plate. Measuring and processing methods for this experiment are described in [24-26].

The distribution of x-coordinate of the reconstructed vertex in target is shown in Fig.2. This distribution has a clear two-peaks structure, that corresponds to the position of the interaction vertex inside either lexan or lead plate. The vertex reconstruction accuracy was 0.025 cm.

The neutral strange particles were observed through charged decay modes; four kinematical hypotheses were tried for each V°:

$$K_s^\circ \longrightarrow \pi^+ + \pi^-$$
$$\Lambda \longrightarrow p + \pi^-$$
$$\bar{\Lambda} \longrightarrow \bar{p} + \pi^+$$
$$\gamma \longrightarrow e^+ + e^- .$$

No attempts have been made to separate Λ ($\bar{\Lambda}$) from Σ^0 ($\bar{\Sigma^0}$) production.

The χ^2 distributions for the K_s°, Λ and γ 3-C fit events, are shown in Fig.3. The experimental distributions are in good agreement with the theoretical curves.

Some events (and vees) were rejected during measurements and processing. The major types of the rejected events/vees were :

- unreconstructed events with several tracks coming from the target but not from the primary vertex, so the reconstructed vertex position errors were unsatisfactory;
- high-multiplicity events with the big number of unreconstructed tracks;
- γ–quants with low energy (E<20 MeV/c);
- vees with short tracks, that could not be reconstructed accurately.

We have estimated the efficiency of our measuring and processing methods at the level of 80 %.

From the 2743 reconstructed vees, we have obtained 2659 three - constraint (3C) fits corresponding to a 1915 unique and 744 ambiguous 3C V°'s. The remaining 84 vees with a 1C fit or no fit at all, were those who were not associated with the reconstructed primary interaction and excluded from the analysis. Most of the 1–C fit hypotheses were γ–quants.

After the kinematical fit, about 28 % of the vees had more than one hypotheses. Some standard methods were applied to this set of V°'s to identify ambiguities. The classification of V°s was based on ionization data as well as kinematical fit results.

During the geometrical reconstruction the decay tracks were assumed as p, $\bar{p}$, $\pi^{\pm}$ and $e^{\pm}$. The bubble densities on the tracks of each vee event, were compared with the geometrical program data. We were able to distinguish electrons, pions and protons in the momentum range P<1.5 GeV/c and for *dip* angles less than 65 degrees. More than half of the ambiguous vees became resolvable using ionization data.

To classify the remaining 14 % of the ambiguities, we compared χ^2–probabilities of the hypotheses for the given vee. A hypothesis was rejected if its χ^2–probability was 0.1 of the other hypothesis. Table Ia shows the number of unique and ambiguous events obtained after classification on ionization data and probability cuts. About 9 % of all the vees were still remained kinematically ambiguous.

In Table Ib all the major types of ambiguities we came across between neutral particles, are presented. For these vees, the transverse momentum distribution of the negative decay track (relative to the V°–direction) was used to assign ambiguous vees into the correct class of particles [27, 28]. In Figs. 4a-c we show the $P_T{}^{(-)}$ distributions for all 3C fits V° inside the fiducial volume. The maximum $P_T{}^{(-)}$ values for Λ and K_s° :

$P_T{}^{max} = 0.100\ GeV/c$, and $P_T{}^{max} = 0.206\ GeV/c$.

The theoretical distributions of $P_T{}^{(-)}$ for the decay particles [27, 28] is described as :

$$dN = \frac{P_T{}^{(-)} dP_T}{P_T{}^{max}(P_T{}^{max2} - P_T{}^{(-)^2})^{1/2}} .$$

The γ's were easily removed from the neutral strange particle hypotheses, as soon as the region with $P_T{}^{(-)}$<0.01 GeV/c contains 98% of unique gammas and only 2% of V°–particles; therefore the ambiguous decays V°/γ were taken as γ's in that region.

The event fitting both: the Λ and K_s° hypotheses, was assigned to the Λ channel if $P_T{}^{(-)}$<0.11 GeV/c. Figure 4a shows the $P_T{}^{(-)}$ distribution obtained before the classification procedure for the sum of unique and ambiguous K_s°. Fig.4b shows the same distribution for unique K_s°–events, and 4c – for unique Λ–events. It is seen that the deviation from the expected distribution for K_s° (shaded area in Fig. 4a) was obviously coming from the admixture of Λ - particles and then disappeared after the ambiguity selection. The results of applying of $P_T{}^{(-)}$ criterion to the ambiguous vees are also presented in Table Ib.

To check the accuracy of the geometrical reconstruction, the effective masses of K_s°, Λ and $\bar{\Lambda}$ were calculated from the measured momenta of the decay products. They were found as : 0.496±0.012 MeV for K_s°, and 1.116±0.004 MeV for (Λ+$\bar{\Lambda}$) . The effective mass distributions for K_s° and (Λ+$\bar{\Lambda}$) are shown in Fig.5.

All V°s were assigned a geometrical weight factor to take into consideration the correction for the loss of decays outside the fiducial volume and for loss of particles decaying near the production vertex. The weight factor

$$W_{geom} = 1/(e^{-(L_{min}/D)} - e^{(-L_{pot}/D)})$$

is the inverse probability to observe potentially the vee. L_{min} is the minimal acceptable value for the distance between the interaction vertex and the decay vertex of the V°; L_{pot} is the potential path along the line of flight of a neutral particle from the production vertex to the boundary of the fiducial volume. For the strange particles $D = c * \tau(p/m)$, where p, m and τ are the measured momentum, the mass, and the lifetime of

V°. For γ-quants D is the conversion length which was calculated using formulas in [29].

The distributions of x, y and z coordinates of the V°/γ vertices are shown in Fig.6. The following cuts were made on values of fiducial volume bounds:

$$11.6cm < x < 75.6cm$$

$$-8.5cm < y < 17.5cm$$

$$-42.5cm < z < -13.5cm.$$

To check a possible loss of V°s close to the primary vertex, the number of events weighted with a geometrical weight, were plotted versus minimum cut values L_{min}. It could be seen from Fig.7 that the value of the weighted number of events, at first, increases while L_{min} growing, then at some value it stops to increase. This value is considered as the best cut-off value for L_{min}.

With these cuts we loose 13% of all the vees : 9% of the vees were outside fiducial volume and 4% of the vees were rejected due to L_{min} cuts.

The average geometrical weights turned out to be: 1.43 for K°_s, 1.39 for Λ, and 1.42 for $\bar{\Lambda}$.

Corrections were also made for the unseen neutral decay modes of the V°s by multiplying the geometrical weight to factor $W_{br} = 1/B$, where B is the branching ratio for the visible decay mode of the V°. For γ the value of B is 1.0.

Weight factor W_{sr} was also introduced to take care of losses in scanning and reconstruction. Finally, every V° was weighted by a factor $W_{tot} = W_{geom} * W_{br} * W_{sr}$. In Fig.8 the distributions of the mean total weights W_{tot} for different charged multiplicities n_{ch} associated with a K°_s and Λ production, are shown.

The total numbers of the registered events and measured vees together with the corrected (weighted and with the identified ambiguities), number of V°s are presented in Table II. This is our final statistics used for the further analysis.

4. Beam contamination and systematic errors

Beam contamination with negative π^- mesons was an obvious source of systematic errors in our experiment. The contribution from the background interactions was accounted using both : data extrapolating on strange particle production in π^--nuclei interactions at close energies, and the Monte-Carlo simulated π^--nuclei events at 12.2 GeV/c, obtained with FRITIOF code [30]. The contribution of V° from the background events could reach even 40% for lead, and it was the reason of the bigger uncertainties in our final results we had expected.

To verify the π^--nuclei data obtained at 12.2 GeV/c, we have used this code to simulate also the π^-–C and π^-–Pb interactions at 5 and 40 GeV/c. Then they were compared with the existing experimental data at these energies, and good agreement was found for characteristics of V°'s [31] as well as the charged particles [32].

The absolute value for beam contamination was obtained with the method previously used for $\bar{d}p$– and $\bar{d}d$–experiments. This method based on comparison of number of events with antiproton-spectator and the number of all inelastic interactions [33]. Thus, for pure antideuteron beam

R_{strip}=N($\bar{d}$+p $\rightarrow \bar{p}_{strip} + X$)/N($\bar{d}$+p $\rightarrow X$) = 0.42±0.03.

For the antideuteron beam with the admixture of π^-–mesons, the ratio of spectator events to all events is lower, and the beam contamination could be estimated from this ratio.

We identified the antiproton-spectator among all the secondary charged particles for $\bar{d}d$– and $\bar{d}A$–interactions. The spectator was a negatively charged particle with a momentum (4.8 – 7.2) GeV/c and with an emission angle $\leq$3 degr. respectively to the incident antideuteron. Obviously, there is some small quantity of fast particles from π^-–p and π^-–d interactions that also could satisfy these conditions, so the probability of "false spectator" $\overline{R_{strip}}$ was taken into account.

The beam contamination was estimated at the level of 1.73 π^- per 1 $\bar{d}$. It means that the number of background interactions could reach 35% of all interactions in deuterium target, 45% for lexan and 50% for lead plates.

As it was mentioned above, the V° production cross sections in π^-A interactions were obtained using the both : interpolation of existing experimental data and FRITIOF simulated events. The total inelastic cross sections for π^-C, π^-Pb, $\bar{d}$C and $\bar{d}$Pb interactions at 12.2 GeV/c were also obtained from experimental data [34, 35] and simple Glauber-type calculations using DIAGEN code [36]. All these quantities were coefficients in a system of linear equations we had to solve to subtract the background processes and obtain V° yields in real $\bar{d}$d, $\bar{d}$C and $\bar{d}$Pb interactions. In Fig.9 all the quantities used in these equations are shown.

All the known values, included into the equations (numbers of events and neutral strange particles, inelastic cross sections, V° production cross sections in π^-–A reactions) are known with some errors. It is not so easy to calculate the errors in the data we obtain, as soon as all the input data and their errors are correlated with each other. That is why we have chosen the following method : the equation system was solved many times, while the input data were varied within the limits of the experimental errors. The output data values were calculated by the average values of the errors found from all the number of the solutions.

The efficiency of measuring and reconstruction procedures depends on the charged particles multiplicity in the primary interactions. The loss probability of the whole event or the definite number of its tracks is higher for the events with a large multiplicity.

Fig.10 presents the comparison of the event multiplicities found while scanning and the multiplicities of the measured and reconstructed events. Really, we have observed some losses of the charged tracks (mostly positive) for high multiplicities. It could be explained by larger number of low-energy and short (stopped) tracks among them, than among the negative ones.

In our further analysis the losses of the events/tracks are accounted for while introducing correction weights for all multiplicities and both signs of the tracks of the primary interaction.

5. Experimental results

Not many results concerning strange particle production on nuclear targets were published :

- $\bar{p}d$ interactions at 1 - 3 GeV/c [3, 4] ;
- the measurements of $\bar{p}$+C, Ti, Ta, Pb at (0–450) MeV/c [5] ;
- the KEK measurements of $\bar{p}$Ta interactions at 4 GeV/c [6, 7] ;
- the streamer chamber measurement of PS 179 experiment at LEAR ($\bar{p}$+He^3, He^4 and Ne^{20} at rest and at 600 MeV/c) [8-12];
- recent results on strange particles production obtained at ITEP ($\bar{p}$–Xe at 0–0.9 GeV/c) [13, 14] ;
- the measurements of ASTERIX ($\bar{p}$+N^{14} at rest) [15].

The obtained results for Λ/K_s° production ratios are listed in Table IIIa. These ratios are directly connected with multi - particle effects in complex nuclei. They also may be indicative of cascading mechanisms which may lead to enhanced Λ-production relative to non-cascading K_s°.

The most striking feature of all the data in Table IIIa is the unexpectedly high Λ–hyperon production yields, compared with $\bar{N}N$data.

For $\bar{p}p$– and $\bar{p}$d – interactions at the same energies, this ratio is smaller for about one order of magnitude : R_{Λ/K_s^0}= 0.2–0.5 at momentum range 4.0–12.0 GeV/c [3, 12].

But in $\bar{p}A$ reactions even for stopping antiprotons, the Λ yield turns out to be high and comparable with the K_s° production cross section.

Obviously, the strangeness enhancement in $\bar{p}A$ reactions is connected with the effect of nuclear medium, and can not be calculated from $\bar{N}N$data using simple geometrical extension. At LEAR energies the production of a Λ on a single nucleon is forbidden (as the threshold for reaction $\bar{p}p \rightarrow \Lambda\bar{\Lambda}$ is p=1435 MeV/c), and several nucleons should be involved into this interaction.

In Table IIIa we have also included the results of $\bar{p}$Xe experiment at 200 GeV/c. At energies higher than few GeV, the Λ production is suppressed due to formation length effects and secondary particles geting out off the nucleus without producing a cascade.

In [21] it was shown that at 12 GeV/c antideuterons (or antinucleons at 6 GeV/c) are very good tools to investigate these effects because at

this energy the antinucleons can penetrate deep enough into a nucleus, and the emitted pions are concentrated in a narrow cone (with the average angle about 10 degrees). Also the ability of antideuterons to produce the higher temperatures into a nucleus due to simultaneous annihilation of the both antinucleons, was predicted in this work.

We were far from the intention to investigate the effects of a "very hot spot" inside a nucleus, as soon as our early antideuteron data had shown that the cross section of the total antideuteron- deuteron annihilation was negligible (about 0.1 mb).

But the antideuteron as a projectile, gives us another interesting opportunity — to mark the peripherical interactions of antinucleons with the nucleus. The deuteron is a weakly-bounded system of a radius comparably smaller than the radius of the heavy nuclei, and when one nucleon (antiproton) does not interact but reveals itself as a fast spectator, another nucleon (antineutron) interacts close to the nuclear surface. We expect that the strangeness production should be somewhat different for these events compared with the central collisions.

We calculated the ratios like

$$R_{K_s^0} = \frac{N(K_s^0)}{N_{inelastic}}$$

$$R_\Lambda = \frac{N(\Lambda) + N(\Sigma^0)}{N_{inelastic}}$$

$$R_{\Lambda/K_s^0} = \frac{N(\Lambda) + N(\Sigma^0)}{N(K_s^0)} \ .$$

The main contribution to our data errors comes from the background extraction procedure.

The observed Λ/K_s° production ratios for antideuteron-nuclei collisions and the same ratios for the events with antiproton– spectator, are shown in Table IIIb. They are close to those ones obtained in $\bar{p}A$ experiments at lower energies. But there is a significant difference between the peripherical and central events.

The yields of K_s° and Λ are presented in Table IV; they depend on target mass, but R(K_s°) yield depends more moderately on A.

We have also observed a dramatic difference in Λ and $\bar{\Lambda}$ productions, especially for the heavy nucleus. The yield ratio $\bar{\Lambda}/\Lambda$ was found as $3 * 10^{-2}$ for lead .

The behavior of neutral strange particles production on target mass, is shown in Fig.11. It is obvious that the dependencies of Λ, K°_s and $\bar{\Lambda}$ yields are different. At the same time, the V°s from peripherical interactions behave very similar. (The statistics for $\bar{\Lambda}$s is insufficient, and the data are not shown for stripping events).

The difference in yields for peripherical and central interactions is very surprising. The Glauber calculations for $\bar{d}$–Pb interactions give us the mean values for impact parameter of antideuteron :

$< b >$=4.6 fm in the case when both antinucleons interact; and

$< b >$=7.5 fm for events with antinucleon spectator — it means that the second nucleon interacts very closely to the edge of the target nucleus. One could suppose that the conditions for Λ's production if they are produced in the secondary rescattering processes, are less favorable in peripherical interactions. At the same time, it should not greatly influence K°_s yields, as K°_s-mesons appeared from primary $\bar{N}N$ interaction.

The number of interactions with fast $\bar{p}$-spectator decreases while target nucleus mass being increased. In our experiment the registered number of these events was 39%, 23% and 11% for deuterium, carbon and lead, correspondingly. It is in good agreement with the Glauber calculations.

One can try to estimate the ratio R_{Λ/K^0_s} for "central" $\bar{d}A$ interactions, when the both antinucleons interact into a nucleus. We have obtained this value for $\bar{d}$Pb reaction subtracting the doubled data for spectator events from all the data. This value is also presented in Table IIIa and turns out to be very close to the value from $\bar{p}$Ta interactions at 4 GeV/c [7].

6. Conclusion

We have studied the neutral strange particle production in antideuteron-nuclei interactions at 12.2 GeV/c. Our results are in agreement with the data from the antiproton experiments at various energies and nuclear targets. Also we can conclude that :

• In $\bar{d}$–nuclei interactions, the Λ production cross section is enhanced.

LEXAN + LEAD				
	no	good	fit	76
K_s°	-	-	-	357
-	Λ	-	-	365
K_s°	Λ	-	-	56
-	-	$\bar{\Lambda}$	-	17
K_s°	-	$\bar{\Lambda}$	-	11
-	Λ	$\bar{\Lambda}$	-	1
-	-	-	γ	777
K_s°	-	-	γ	3
-	Λ	-	γ	6
K_s°	Λ	-	γ	1
-	-	$\bar{\Lambda}$	γ	2
K_s°	-	$\bar{\Lambda}$	γ	1
-	Λ	$\bar{\Lambda}$	γ	0
1467 events (1673 Vees)				
81 ambiguous vees				

DEUTERIUM				
	no	good	fit	8
K_s°	-	-	-	108
-	Λ	-	-	83
K_s°	Λ	-	-	36
-	-	$\bar{\Lambda}$	-	39
K_s°	-	$\bar{\Lambda}$	-	10
-	Λ	$\bar{\Lambda}$	-	2
-	-	-	γ	687
K_s°	-	-	γ	13
-	Λ	-	γ	39
K_s°	Λ	-	γ	4
-	-	$\bar{\Lambda}$	γ	35
K_s°	-	$\bar{\Lambda}$	γ	4
-	Λ	$\bar{\Lambda}$	γ	2
961 events (1070 Vees)				
158 ambiguous vees				

Table Ia. Summary of accepted "pure" and ambiguous hypothesises for V° and γ after classification based on ionization data and probability cuts.

AMBIGUOUS EVENTS					
92	(K_s°,Λ)	$\longrightarrow$	16 K_s°	+	72 Λ
21	$(K_s^\circ,\bar{\Lambda})$	$\longrightarrow$			18 $\bar{\Lambda}$
19	(K_s°,γ)	$\longrightarrow$	6 K_s°	+	13 γ
43	(Λ,γ)	$\longrightarrow$	8 Λ	+	34 γ
37	$(\bar{\Lambda},\gamma)$	$\longrightarrow$	6 $\bar{\Lambda}$	+	31 γ

Table Ib. The pattern of ambiguous 3–C fit hypothesises. Classification of kinematically resolved ambiguities after applying of $P_T^{(-)}$ criterion.

REACTION		Fitted, unweighted	Weighted, corrected
$(\bar{d}+\pi^-)$+d	→ inelastic	7800 scanned	
$(\bar{d}+\pi^-)$+d	→ K°_s+X	106	240
$(\bar{d}+\pi^-)$+d	→ Λ+ X	86	174
$(\bar{d}+\pi^-)$+d	→ $\bar{\Lambda}$+ X	38	72
$(\bar{d}+\pi^-)$+d	→ γ+ X	229	
$(\bar{d}+\pi^-)$+C	→ inelastic	3750 scanned	
$(\bar{d}+\pi^-)$+C	→ K°_s+X	77	167
$(\bar{d}+\pi^-)$+C	→ Λ+ X	59	138
$(\bar{d}+\pi^-)$+C	→ Λ+ X	9	23
$(\bar{d}+\pi^-)$+C	→ γ+ X	308	
$(\bar{d}+\pi^-)$+Pb	→ inelastic	3890 scanned	
$(\bar{d}+\pi^-)$+Pb	→ K°_s+X	204	479
$(\bar{d}+\pi^-)$+Pb	→ Λ+ X	299	597
$(\bar{d}+\pi^-)$+Pb	→ $\bar{\Lambda}$+ X	7	13
$(d+\pi^-)$+Pb	→ γ+ X	656	

Table II. Total number of interactions and number of measured and corrected events in our experiment.

Momentum (GeV/c) (GeV/c)	$\bar{p}$-He	p-Ne	$\bar{p}$ Xe	$\bar{p}$-Ta
at rest	1.09±0.10	1.25±0.19	1.15±0.19	
0.4-0.9			1.57±0.20	
0.6	0.94±0.04	2.3±0.7		
4.0				2.4±0.3
200.0			0.43±0.09	

Table IIIa. Review of production ratios R_{Λ/K^0_s} in $\bar{p}$ Nuclei interactions (Refs. [6-16])

	$\bar{d}$–d	$\bar{d}$–C'	$\bar{d}$–Pb
R_{Λ/K^0_s} all events	0.89±0.17	1.11±0.32	1.98±0.33
R_{Λ/K^0_s} +$\bar{p}$–spectator	0.59±0.23	0.63±0.28	0.93±0.40
R_{Λ/K^0_s} "central" events	.....	.....	2.13±0.83
$R_{\bar{\Lambda}/\Lambda}$ all events	0.68±0.13	0.26±0.09	0.03±0.01

Table IIIb. Production ratios R_{Λ/K^0_s} and $R_{\bar{\Lambda}/\Lambda}$ in $\bar{d}$-Nuclei interactions at 12.2 GeV/c. Background is extracted.

	d	C'	Pb
$R_{K^0_s}$ %	2.57±0.43	4.02±1.16	14.5±4.0
$R_{K^0_s}$ % $\bar{p}$-spectator events	2.37±0.50	4.20±1.37	11.4±3.2
R_Λ %	2.24±0.33	4.25±1.03	27.9±5.0
R_Λ % $\bar{p}$-spectator events	1.40±0.39	2.65±1.09	10.3±3.6
$R_{\bar{\Lambda}}$ %	1.52±0.19	1.10±0.30	0.85±0.24

Table IV. Relative yields of Λ (R_Λ), K°_s ($R_{K^0_s}$) and $\bar{\Lambda}$ ($R_{\bar{\Lambda}}$) (per registered primary interaction in the target). Background is extracted.

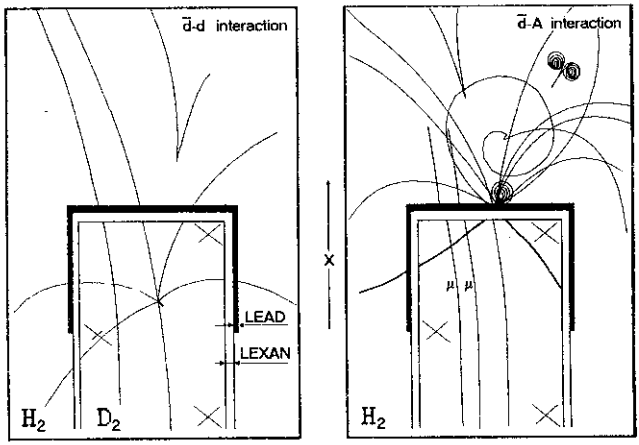

Fig.1. Fully reconstructed $\bar{d}d$ and $\bar{d}A$ events with a V° candidates.

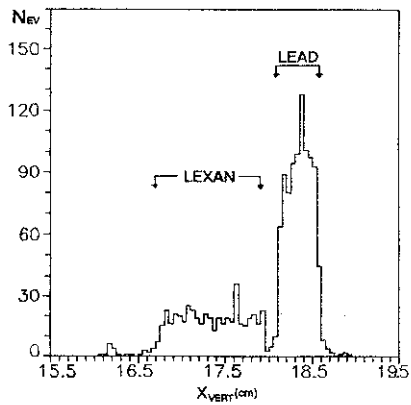

Fig.2. Reconstructed vertex x-coordinate distribution. (Beam aimed along the x-axis).

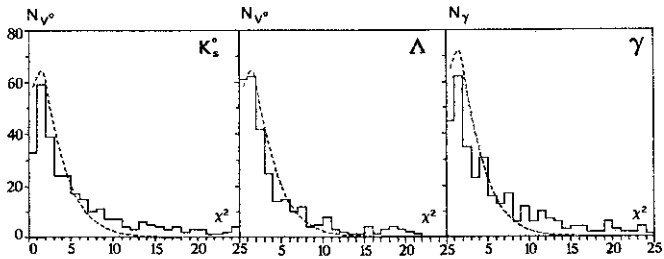

Fig.3. χ^2 distribution for all K_s°, Λ and γ 3-C fit events with no cuts and weights applied (solid line). Dashed line - is the expected theoretical χ^2 curve.

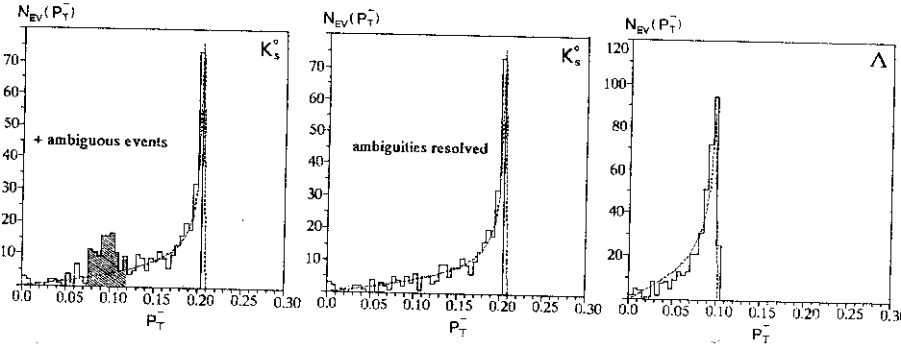

Fig.4. Transverse momentum distribution of the negative decay particle from V° decays. (A) – the sum of unique and ambiguous K_s°. Shaded events are those selected by the $P_T^{(-)}$ cut. (B) and (c) are from unique fits for K_s° and Λ particles.

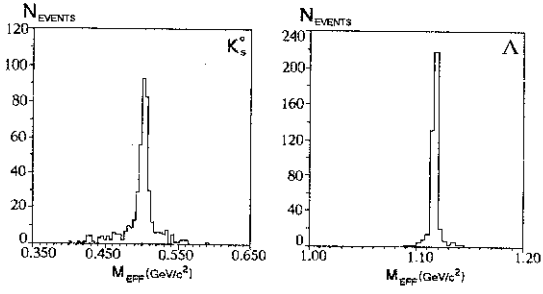

Fig.5. The effective mass distributions for K_s° and $(\Lambda+\bar{\Lambda})$ calculated from the measured momenta of the decay products.

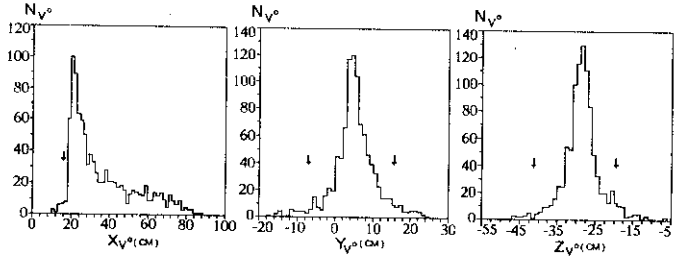

Fig.6. The distributions of x, y and z coordinates of the V°/γ vertices. Arrows indicate the chosen fiducial volume.

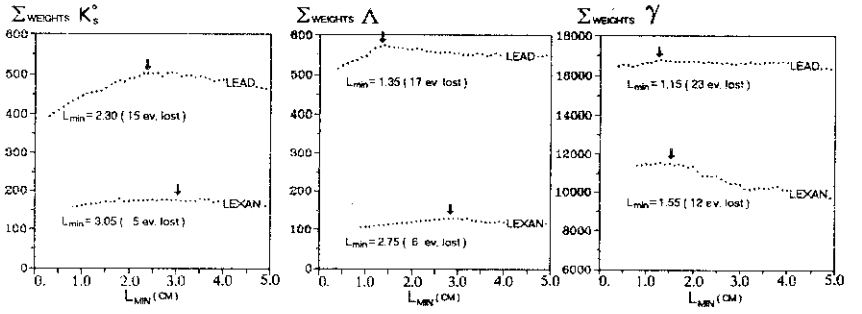

Fig.7. Weighted number of events as a function of minimum length L_{min}. The chosen values of L_{min} are shown with arrows.

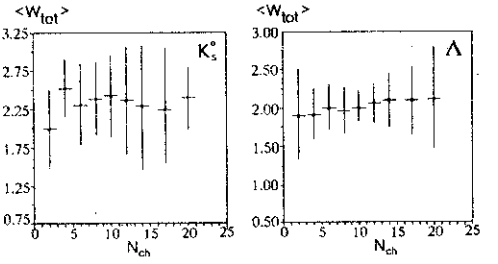

Fig.8. The distributions of the mean total weights W_{tot} for different charged multiplicities n_{ch} at the main interaction vertex associated with a K_s° and Λ production.

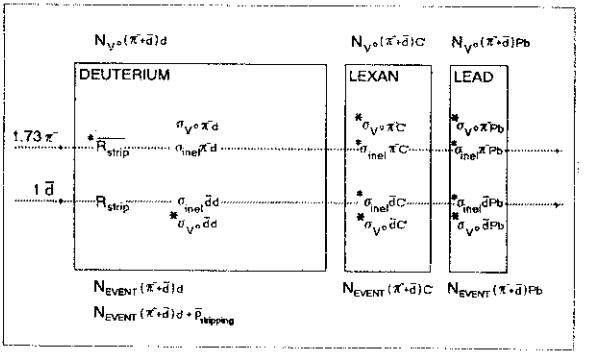

Fig.9. All the values are given schematically : values known from experiment and obtained while modelling. These values were used in background extraction procedure while obtaining the numbers of V°s in $\bar{d}A$ interactions and their errors.

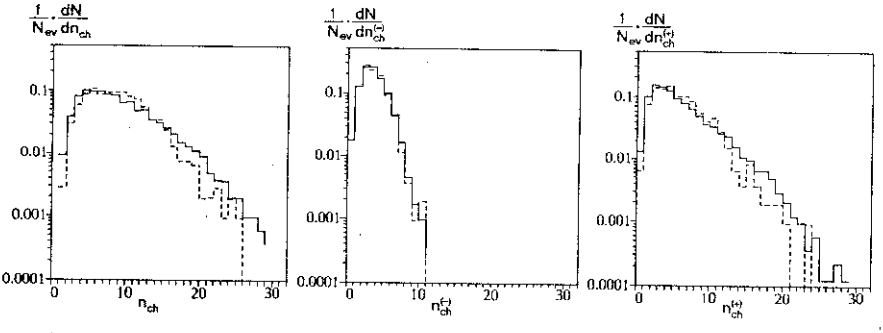

Fig.10. Multiplicity distributions for all the particles, negative and positive ones in $\bar{d}A$–interactions. Scan information for events is represented with solid line; dashed line for events after measuring and processing.

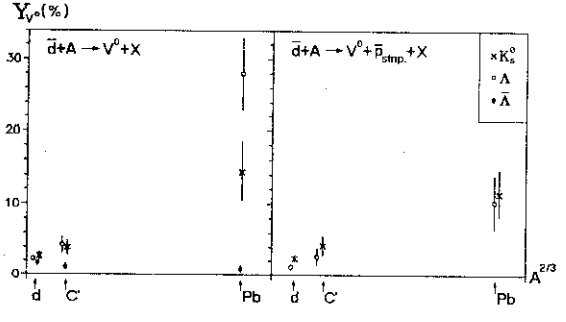

Fig.11. Relative yields of K°_s, Λ and $\bar{\Lambda}$–particles for various nuclear targets in our experiment. Target masses are shown as $A^{2/3}$.

The yield of Λ is almost equal to yield of K_s° even for a deuterium nucleus, but almost equal to 2 in $\bar{d}$Pb interactions. For lead, the Λ production cross section is a substantial part of the total inelastic cross section.

• Our $\bar{d}$–nuclei data supports the conclusion being given in [17] while reviewing $\bar{p}A$–experiments, that the ratios R_{Λ/K_s^0} are almost independent on incident momentum of the projectile. In [20] this feature is referred to as "Λ–saturation".

• The possibility to observe the fast $\bar{p}$-spectator allows one to mark the antinucleon-nucleus interactions of peripherical type, where the contribution of intranuclear cascading processes is lower. The yield of Λ particles in peripherical interactions is suppressed if to be compared with yields in non-peripherical case. At the same time, the "peripherricity" of the interaction does not influence significantly the K_s° yields.

• The dependence of production yields on target mass is different for Λ–, K_s° - and $\bar{\Lambda}$–particles. At the same time, the V° from peripherical interactions behave very similarly.

• The observed difference in relative yields of Λ– particles in antideuteron- deuteron interactions with and without stripping antiproton, may reflect the sufficient role of rescattering processes for Λ production even in the simplest deuteron nucleus in spite of its poor structure.

• The dramatic difference in Λ and $\bar{\Lambda}$ productions in $\bar{d}A$ interaction was observed. The ratio $R_{\Lambda/\bar{\Lambda}}$ turned out to be small: $3 * 10^{-2}$ for lead target.

References

[1] P.Koch, B.Muller, J.Rafelski, Phys.Rep. 142 (1986) 168.

[2] J.Rafelski, Phys.Lett. 207B (1988) 371.

[3] B.Y.Oh et al., Nucl.Phys. B51 (1973) 57.

[4] S.J.H.Parkin et al., Nucl.Phys. B277 (1986) 634.

[5] G.T.Condo et al., Phys.Rev. C29 (1984), 1531.

[6] K.Miyano et al., Phys.Rev.Lett. 53 (1984) 1725.

[7] K.Miyano et al., Phys.Rev. C38 (1988) 2788.

[8] Yu.A.Batusov et al., JINR E1-90-118, Dubna, 1990.
[9] Yu.A.Batusov et al., JINR Rapid Comm. 7 (1988) 24.
[10] Yu.A.Batusov et al., Yad.Fiz. 50 (1989) 1524.
[11] F.Balestra et al., Phys.Lett. B194 (1987), 192.
[12] F.Balestra et al., Nucl.Phys. A526 (1991) 415.
[13] A.D.Andryakov et al., prepr. ITEP 104-90, Moscow, 1990.
[14] A.Dolgolenko, in Proc. of Workshop on Nucleon-Antinucleon Interactions, Moscow, 1991, Yad.Fiz. 55 (1992) 1253.
[15] J.Riedlberger et al., Phys.Rev. C40 (1989) 2717.
[16] I.Derado et al., Z.Phys.C - Particles and Fields, 50 (1991) 31.
[17] C.Guaraldo, Nuovo Cim. 102A (1989) 1137.
[18] J.Cugnon, J.Vandermeulen, Phys.Rev. C39 (1989) 181.
[19] C.B.Dover, P.Koch, prepr. BNL-42105 (1988).
[20] D.E.Kharzeev, M.G.Sapozhnikov, JINR E4-88-930, Dubna, 1988.
[21] D.Strottman, W.R.Gibbs, Phys.Lett. 149B (1984) 288.
[22] V.V.Vasiliev et al., in Proc. of 11th Int.Conf. on High Energy Accelerators, Geneva, 1980, p.361.
[23] Antipov Yu.M. et al., Yad.Fiz. 13 (1971) 135.
[24] B.V.Batynia et al., JINR, P1-89-519, Dubna, 1989.
[25] D.Bruncko et al., JINR B1-91-101, Dubna, 1991.
[26] D.Bruncko et al., JINR B1-91-102, Dubna, 1991.
[27] K.Jaeger et al., Phys.Rev. D11 (1975) 1756.
[28] B.Batyunya et al., JINR 1-11194, Dubna, 1978.
[29] V.G.Grishin, JINR P2636, Dubna, 1966.
[30] B.Andersson et al., Nucl.Phys. B281 (1987) 289.
B.Nillson-Almquist, E.Stenlund, Comp.Phys.Comm. 43 (1987) 387.
[31] N.S.Amaglobeli et al., JINR P1-9513, Dubna, 1975.; L.L.Gabunia et al., Yad.Fiz. 50 (1989) 1035. ; N.S.Angelov et al., Yad.Fiz. 24 (1976) 732.; N.S.Angelov et al., JINR P1-9648, Dubna, 1976.
[32] N.S.Angelov et al., Yad.Fiz. 25 (1977) 1013. ; N.S.Angelov et al., JINR P1-11293, Dubna, 1978.
[33] I.M.Gramenitsky et al., JINR 1-84-788, Dubna, 1984.
[34] Bobchenko B.M. et al., Yad.Fiz. 30 (1979) 1553.
[35] Vlasov A.B. et al., Yad.Fiz. 27 (1978) 413.
[36] S.Yu.Schmakov et al., Comp.Phys.Comm. 54 (1989) 125.

Received by Publishing Department
in January 25, 1993.